# Modeling and Semi-Physical Simulation Validation for the Hydrogen Supply System in Proton Exchange Membrane Fuel Cell

*Xiaosong Song[1], Zhe Dong[2*], Weiye Sun[3], Ningyong Liu[4],Yi Zhang[5]*

*North China University of Technology, Shijingshan District, Beijing, China*
**dongzhe@ncut.edu.cn*

**Keywords**: FUEL CELL, HYDROGEN SUPPLY SYSTEM MODELING, MIXED GAS, SEMI-PHYSICAL SIMULATION

## Abstract

To meet the demands for precise control and rapid iteration of the hydrogen Loop in Proton Exchange Membrane Fuel Cell (PEMFC) systems, this paper constructs a complete high-precision hydrogen supply system model and verifies it through semi-physical simulation. By developing a hydrogen supply system model that encompasses the composition, flow, and reaction characteristics of the mixed gas, the dynamic behavior of the hydrogen supply system is comprehensively simulated. In addition, a semi-physical simulation platform with real-time data interaction capabilities is established to accurately replicate the actual operating conditions of the fuel cell. The research results show that the established model can effectively reflect the dynamic response characteristics of the hydrogen supply system, providing strong technical support for the design and verification of PEMFC control strategies. This work is of great significance for promoting the engineering application of fuel cells in the field of clean energy.

## 1 Introduction

Driven by energy transition and dual carbon goals, traditional fossil fuel-based energy systems are shifting to clean, low-carbon alternatives due to high emissions and resource limitations [1]. Fuel cells, which efficiently convert chemical energy to electricity, are emerging as a core technology for future energy needs. They offer advantages such as fast start-up, modular design, and zero-carbon emissions. Unlike intermittent renewables like solar and wind, fuel cells provide stable power, making them ideal for long-term energy storage and high-power applications [2, 3].

Fuel cells consist of hydrogen, air, and thermal management systems. The hydrogen supply system's dynamics significantly impact fuel cell lifespan and efficiency, making accurate modeling and simulation essential for understanding its behavior. Zhu et al. [4] developed a multidimensional nonlinear MIMO model for the hydrogen supply system, considering hydrogen/nitrogen permeation and water migration. Their analysis of the relative gain array revealed the coupling between pressure and hydrogen supply variables, providing insights into the multivariable interactions. Qing et al. [5] developed a dynamic model for the hydrogen recirculation system using piecewise linearization to address the nonlinearities of the ejector and pump. This method simplifies the model and enhances computational efficiency. Quan et al. [6] modeled the fuel cell hydrogen supply system using the ideal gas law and linearized state-space equations. It is intuitive and suitable for fast analysis when high precision is not required. Xu et al. [7] built a machine learning model for predicting ejector performance in PEMFC hydrogen supply systems using data from 20 fuel cell stacks. It is highly accurate in specific scenarios but relies heavily on data. Qin et al. [8] developed a PEMFC hydrogen supply system model based on an ejector, incorporating electrochemical reactions, gas supply manifolds, and the ejector itself. By establishing flow relationships through entrainment ratios and describing pressure dynamics via mass conservation, the model provides a multi-component coupled modeling method for control, offering a comprehensive basis for system control studies. Hauck et al. [9] modeled the PEMFC anode recirculation system with three control volumes. It tracks pressure dynamics and includes nitrogen diffusion and purge flow models, supporting model predictive control. Nikiforow et al. [10] designed an ejector-based hydrogen supply system for a 5kW PEMFC system, validated by a 2D Computational Fluid Dynamics(CFD) model. However, its high computational cost restricts its application in resource-limited settings. Li et al. [11] modeled a hydrogen supply system in AMESim, covering key components like the anode chamber and ejector. The model tracks pressure dynamics through mass conservation but has limitations in platform dependency and scalability.

Most fuel cell studies simplify the hydrogen supply system as a single-gas system, ignoring impurities like nitrogen and water vapor, leading to inaccurate models. Additionally, key actuators are often modeled linearly and statically, without considering response delays or nonlinear coupling. These limitations impede the development of effective control algorithms and performance optimization.This study addresses the aforementioned issues by developing a complete high-precision hydrogen supply system model.The main contributions are:

1)Considers mixed gas characteristics in the hydrogen supply system, accurately simulating flow, transport, and reaction.

2)Modeling key components (proportional valves, ejectors, pumps, and valves) with mechanical response delays and fluid dynamics, providing a basis for optimized control.
3)Designs a semi-physical simulation platform with modular interfaces for data interaction between virtual models and physical controllers, closely mimicking real physical systems.

## 2. Mixed Gas and Chamber Modeling

This section develops mixed gas and chamber models to capture dynamics affecting key parameters like pressure and reaction rates in fuel cell systems, forming the basis for a high-precision hydrogen supply system model.

### *2.1 Mixed gas model*

This paper uses the NASA polynomial model for the temperature-dependent specific heat capacity [12] and the ideal gas assumption to describe gas energy transfer and state changes. The constant-pressure specific heat capacity $c_{pm}$ is given by:

$$\frac{c_{pm}}{R} = a_1 + a_2T + a_3T^2 + a_4T^3 + a_5T^4 \quad (1)$$

where $R$ is the gas constant, $T$ is the gas temperature, and $a_1, a_2, a_3, a_4, a_5$ are fitting coefficients from the NASA thermodynamic database, The fitting parameters for gases in the temperature range of 298~1000 $K$ are shown in Table I.

TABLE I: Gas fitting parameters

| | $a_1$ | $a_2$ | $a_3$ | $a_4$ | $a_5$ |
|---|---|---|---|---|---|
| $H_2$ | 2.971 | 3.37e-3 | -7.324e-6 | 6.58e-9 | -1.991e-12 |
| $N_2$ | 3.531 | -1.236e-4 | -5.029e-7 | 2.435e-9 | -1.4088e-12 |
| $H_2O$ | 4.198 | -2.036e-3 | 6.52e-3 | -5.487e-9 | 1.77197e-12 |

For an ideal gas, after mixing different components,the total mass is:

$$M_{total} = \sum_i^N m_i \quad (2)$$

where $m_i$ is the mass of substance $i$.
The mass fraction of each substance $r_{Mass_i}$ in the mixed gas is given by:

$$r_{Mass_i} = \frac{m_i}{m_{total}} \quad (3)$$

The molar fraction of each substance $r_{Molar_i}$ in the mixed gas is given by:

$$r_{Molar_i} = \frac{r_{Mas\ i}}{M_i \sum_i^N \frac{r_{Mass_i}}{M_i}} \quad (4)$$

where $M_i$ is the molar mass of substance $i$.
The gas constant of the mixed gas $R_{mix}$ is:

$$R_{mix} = \sum_i^N r_{Molar_i} * \frac{R}{M_i} \quad (5)$$

The specific heat capacity of the mixed gas $c_{p,mix}$ is:

$$c_{p,mix} = \sum_i^N r_{Mass_i} * c_{p,i} \quad (6)$$

where $c_{p,i}$ is the specific heat capacity of substance $i$.

### *2.2 Chamber model*

The chamber model simulates fluid system capacitance, dynamically calculating pressure, temperature, and gas composition changes. It captures mass accumulation and energy buffering during gas flow, accurately representing the system's inertial dynamics.
Assuming the initial state is pure hydrogen, the total mass of the gas $m_0$ in the chamber can be calculated using the chamber volume $V_{cv}$:

$$m_0 = \rho_{H_2} * V_{cv} \quad (7)$$

Where $\rho_{H_2}$ represents the density of hydrogen gas.
The gas in the chamber follows mass conservation. The change in mass equals the inflow rate minus the downstream feedback rate:

$$\frac{dm_i}{dt} = \sum_{j=0}^N \dot{m}_{j,i,in} - \sum_{j=0}^N \dot{m}_{j,i,out} \quad (8)$$

where $j$ represents the inlet and outlet interfaces of the chamber. The composition of the gas in the chamber at any given time can be calculated using equation (3).
The overall mass change of the gas in the chamber is:

$$m_{cv} = \sum \Delta m_i \quad (9)$$

where $\Delta m_i$ represents the mass change of substance $i$ within the chamber, which is calculated using Equation (8).
Neglecting the kinetic and potential energy of the gas, the energy conservation of the system can be expressed as:

$$\frac{d}{dt} m_{cv}u = Q_{cv} + \sum \dot{m}_{in}h_{in} - \sum \dot{m}_{out}h_{out} \quad (10)$$

where $u$ is the specific internal energy, $Q_{cv}$ represents heat exchange and work done, $h_{in}$, $h_{out}$ are the specific enthalpies of the input and output gas.
For an ideal gas, the relationship between temperature and enthalpy and internal energy is given by:

$$\begin{cases} h = u + pV = u + RT \\ c_p = \frac{dh}{dT} \\ c_v = \frac{du}{dT} = c_p - R_{mix,cv} \end{cases} \quad (11)$$

where $c_p, c_v$ represent the gas's constant-pressure specific heat capacity and constant-volume specific heat capacity, respectively.
Assuming no external heat exchange and work done, the temperature dynamics can be calculated by substituting into the given equation (10):

$$\frac{dT_{cv}}{dt} c_v m_{cv} = \sum \dot{m}_{in}c_{p,in}T_{in} - \sum \dot{m}_{out}c_{p,out}T_{out}$$

$$-\frac{dm_{cv}}{dt}c_v T_{out} \tag{12}$$

The pressure inside the chamber can be calculated using the ideal gas law:

$$p_{cv} = \frac{m_{cv} v_{cv}}{R_{cv} T_{cv}} \tag{13}$$

The pressure at the chamber's outlet is modeled using a first-order low-pass filter to simulate the dynamic response of pressure changes, which can be expressed as:

$$\tau_1 \frac{dp_{out}}{dt} + p_{out} = p_{cv} \tag{14}$$

where $\tau_1$ is the pressure time constant.

## 3 Hydrogen Supply System Modeling

Key components like proportional valve, ejector, and hydrogen pump affect system efficiency, Accurate hydrogen supply system modeling is crucial for control studies. This chapter explores hydrogen supply system modeling, the overall structure is shown in Figure 1.

### *3.1 Proportional valve model*

The proportional valve model follows orifice flow characteristics, with the effective flow area adjusting dynamically based on valve opening to control fluid flow. The proportional valve model established in this paper mainly includes valve mechanical response and flow calculation.The dynamic process of the mechanical response can be described as:

$$\tau_2 \frac{dy_{act}}{dt} + y_{act} = y_{tgt} \tag{15}$$

where $\tau_2$ is the mechanical time constant, $y_{act}$ is the actual valve opening value,$y_{tgt}$ is the target valve opening value.
Internal flow $\dot{m}_{prop}$ can be calculated using the orifice model, which is given by the formula:

$$\dot{m}_{prop} = C * A_1 y_{act} C_1 p_{up} \sqrt{T_{up} R_{H_2}} \tag{16}$$

where $C_1$ is the Proportional Valve flow coefficient, $A_1$ is the area when the Proportional valve is fully open, $p_{up}$, $T_{up}$ are the upstream pressure and temperature, $R_{H_2}$ is the gas constant for hydrogen, and $C$ is a correction coefficient affected by the pressure ratio between the upstream and downstream, which is expressed as:

$$C = \begin{cases} \sqrt{\gamma \left(\frac{2}{\gamma+1}\right)^{\frac{\gamma+1}{\gamma-1}}} & PR < PR_{cr} \\ \sqrt{\frac{2\gamma}{\gamma-1}\left(1 - PR^{\frac{\gamma-1}{\gamma}}\right) \cdot PR^{\frac{1}{\gamma}}} & PR > PR_{cr} \end{cases} \tag{17}$$

where $PR$ is the ratio of the upstream inlet pressure $p_{up}$ to the anode inlet pressure $p_{an,in}$of the fuel cell stack, and $PR_{cr}$ is the critical pressure ratio, which can be calculated using equations (18) and (19), respectively:

$$PR = \frac{p_{an,in}}{p_{up}} \tag{18}$$

$$PR_{cr} = \left(\frac{2}{\gamma+1}\right)^{\frac{\gamma}{\gamma+1}} \tag{19}$$

The isentropic exponent $\gamma$ can be expressed as:

$$\gamma = \frac{c_p}{c_v} \tag{20}$$

The outlet flow rate of the valve $\dot{m}_{prop,out}$ can be expressed as:

$$\tau_3 \frac{d\dot{m}_{prop,out}}{dt} + \dot{m}_{prop,out} = \dot{m}_{prop,out} \tag{21}$$

where $\tau_3$ is the massflow time constant.

### *3.2 Ejector model*

The gas from the proportional valve forms a high-speed jet through the ejector's nozzle, creating a low-pressure zone that draws in gas from the secondary inlet. The secondary inlet mass flow rate $\dot{m}_s$ can be expressed as:

$$\dot{m}_s = \dot{m}_p * ER \tag{22}$$

where $\dot{m}_p$ is the mass flow rate at the primary inlet, and $ER$ is the entrainment ratio.
The outlet mass flow rate is the sum of the primary and secondary flows:

$$\dot{m}_{ejector,out} = \sum \left(\dot{m}_p * r_{Mass_p}\right) + \dot{m}_s * r_{Mass_s} \tag{23}$$

where $r_{Mass_p}$, $r_{Mass_s}$ are the components at the primary and secondary inlets, respectively, and $\dot{m}_{ejector,out}$ is the mass flow rate at the ejector outlet.

### *3.3 Hydrogen recirculation pump model*

The hydrogen recirculation pump in fuel cell systems returns unreacted hydrogen to the anode, reducing waste and ensuring stable operation. It includes a motor model and fluid dynamics model.
The dynamic response of the recirculation pump's motor speed can be simulated by equation (24):

$$\tau_2 \frac{dn_{act}}{dt} + n_{act} = n_{tgt} \tag{24}$$

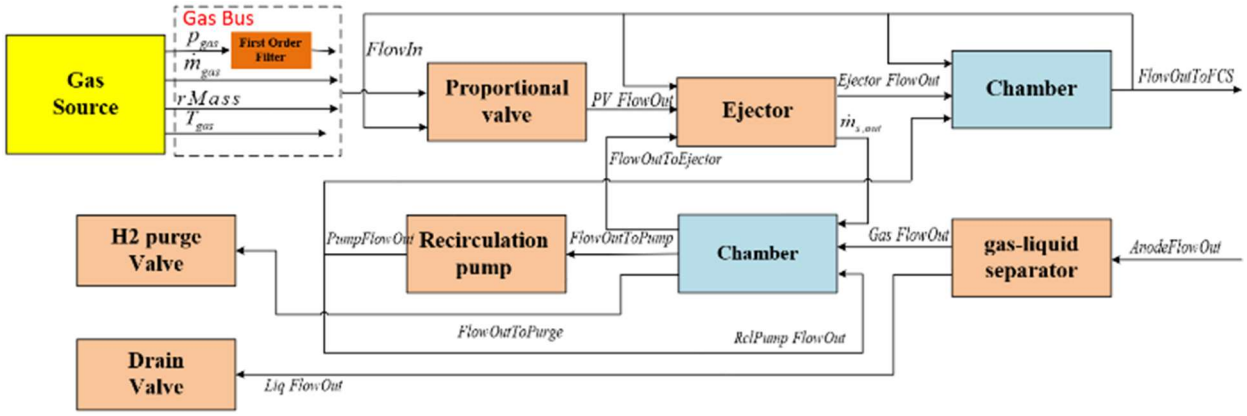


Fig. 1: Overall structure diagram of the supply system

The fluid dynamics model calculates the hydrogen recirculation pump's flow and temperature rise based on speed and pressure differential. Using experimental data and calibration curves (Figures 2a and 2b), a multidimensional mapping relationship is established.

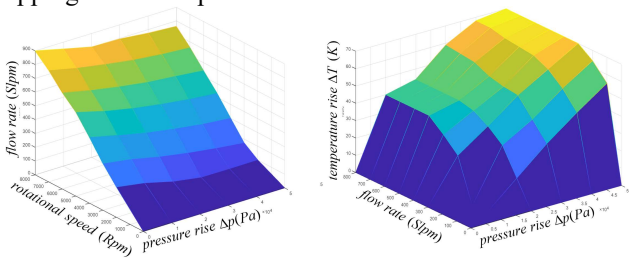


(a) Recirculation pump flow map diagram

(b)Recirculation pump temperature map diagram

Fig. 2: recirculation pump performance maps

$$\dot{m}_{pump} = f(\Delta p, n_{act}) \tag{25}$$

$$\Delta T = f(\Delta p, \dot{m}_{pump}) \tag{26}$$

The pressure differential is calculated by subtracting the gas pressure at the stack outlet leading to the pump $p_{an,out,pump}$ from the anode inlet pressure $p_{an,in}$:

$$\Delta p = p_{an,in} - p_{an,out,pump} \tag{27}$$

The outlet gas flow rate is:

$$\tau_3 \frac{d\dot{m}_{pump,out}}{dt} + \dot{m}_{pump,out} = \dot{m}_{pump} \tag{28}$$

The outlet gas temperature is:

$$T_{pump,out} = T_{pump,in} + \Delta T \tag{29}$$

where $T_{pump,in}$ represents the inlet temperature of the gas.

*3.4 Gas-liquid separator model*

The gas-liquid separator model removes water from hydrogen or air to ensure smooth gas flow and prevent water from entering the fuel cell stack, which could degrade performance. Assuming the gas-water separator operates adiabatically with $T_{out} = T_{in}$. The water separation efficiency can be correlated with the mass flow rate of anode gas at the fuel cell outlet:

$$\eta[0 - 100\%] = f(\dot{m}_{an,out}) \tag{30}$$

The mass flow rate of the separated liquid water can be expressed as:

$$\dot{m}_{liq,out} = \eta * \dot{m}_{an,out} * r_{Mass_{an,H_2O,out}} \tag{31}$$

The composition of the gas changes after separation and can be calculated using equations (2) and (3). The mass flow rate of the separated gas is expressed as equation (32):

$$\dot{m}_{gas,out} = \dot{m}_{an,out} - \dot{m}_{liq,out} \tag{32}$$

*3.5 Water drain and hydrogen purge valve model*

In this study, the water drain and hydrogen purge valves are modeled as open or closed. Their dynamics are described using the orifice model. When the water drain valve is open, the outlet flow rate is:

$$\dot{m}_{drain} = A_2 C_2 \sqrt{2\rho_{H_2O}\Delta p} \tag{33}$$

where $A_2$ is the full-open area of the water drain valve, $C_2$ is the Drain valve flow coefficient, $\rho_{H_2O}$ is the density of water, and $\Delta p$ is the pressure drop between the inlet and outlet, calculated by subtracting atmospheric pressure from the inlet liquid pressure.

$$\dot{m}_{purge} = A_3 C_3 p_{gas,in} \sqrt{T_{gas,in} R_{H_2}} * fac \tag{34}$$

where $A_3$ is the full-open area of the hydrogen purge valve, $C_3$ is the purge valve flow coefficient, $p_{gas,in}$ and $T_{gas,in}$ are the inlet pressure and temperature from the chamber calculations.The correction coefficient $fac$ is calculated using equation (17), with upstream pressure from the anode outlet and downstream pressure as atmospheric.

## 4 Design of the Semi-physical Simulation Platform and Validation of the Model Results

### *4.1 Design of semi-physical simulation platform*

This paper has constructed a semi-physical simulation platform to validate the developed model, as shown in Figure 3. The simulation platform is built based on the RT-Linux operating system, and high-precision real-time interaction is achieved through the co-design of hardware and software. The system employs a modular hardware architecture, equipped with various types of signal interface boards to accurately simulate the electrical characteristics of key components in the fuel cell system, such as valves, sensors, and water pumps.

Based on the module-level Target Language Compiler (TLC) files, the hardware interfaces are standardized and encapsulated to form a visual functional module library in the Matlab/Simulink environment. By using graphical drag-and-drop, dynamic mapping relationships between physical quantities such as pressure, temperature, and rotational speed and hardware channels are established, enabling electrical interaction between virtual devices and real controllers.

The developed fuel cell model is integrated through a rapid control prototyping toolchain based on the X86 architecture. Using RTW code, the physical object model and interface model are synchronously converted into C/C++ code, and an appropriate Makefile compilation script is automatically generated. After cross-compilation, an executable file that can be scheduled on the RT-Linux system is generated. A daemon process is used to automatically deploy the file and switch processes. The system also integrates XCP communication, supporting parallel monitoring and optimization of multiple parameters.

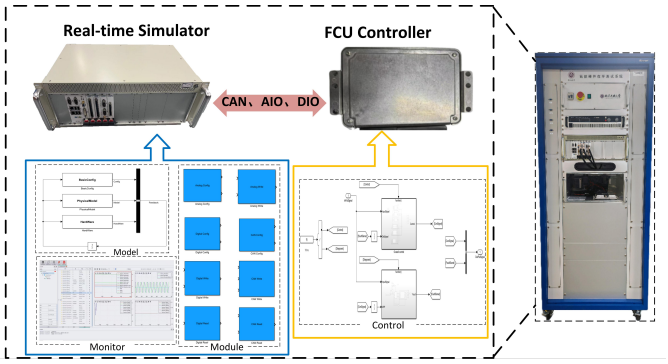


Fig. 3: Experimental verification platform for fuel cell systems

### *4.2 Validation of model effectiveness and rationality*

To validate the constructed model, this paper designs a fundamental control strategy. During system operation, the system first calculates the deviation between the target and actual hydrogen pressure. Subsequently, it dynamically adjusts the PID control parameters based on the pressure difference and load conditions. Additionally, the system dynamically compensates for the proportional valve opening according to the system status and the state of the hydrogen and water drainage valves. The hydrogen recirculation pump adjusts its speed in response to system status, hydrogen pressure, and load requests, while the hydrogen and water drainage valves control their on-off timing based on load requests.

The parameters for the hydrogen supply system are shown in Table II. By varying the current density to simulate load changes, the fuel cell's performance under different loads is tested. As seen in Figure 4, the overall flow rate increases with the load, demonstrating the hydrogen supply system's ability to adjust hydrogen supply and recirculation according to demand.

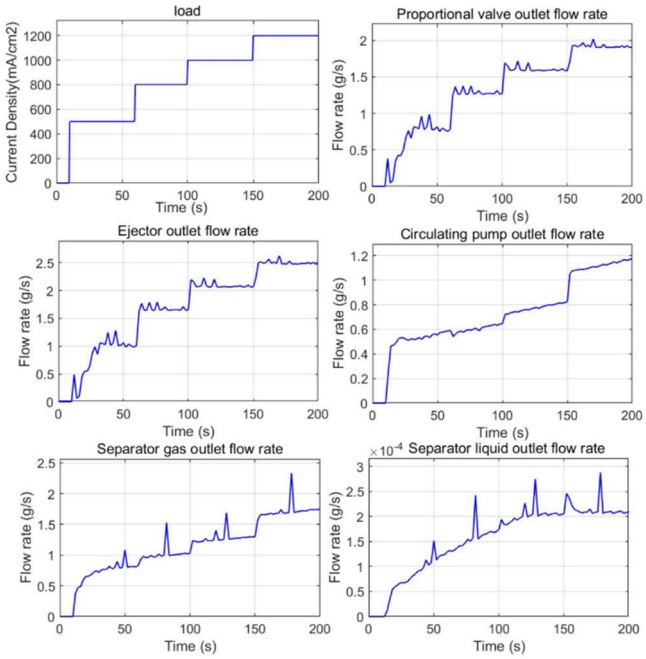


Fig. 4: Flow curves of supply system components

TABLE II: Parameters

| Parame | Value | Description |
|---|---|---|
| $\tau_1$ | 0.1 | Pressure time constant |
| $\tau_2$ | 0.5 | Mechanical time constant |
| $\tau_3$ | 0.2 | Massflow time constant |
| $V_{cv}$ | $600cm^2$ | Cavity volume |
| $ER$ | 0.3 | Ejector ratio |
| $C_1$ | 0.3 | Prop valve Flow coefficient |
| $C_2$ | 0.5 | Drain valve Flow coefficient |
| $C_3$ | 0.3 | Purge valve Flow coefficient |
| $A_1$ | 0.0615 $cm^2$ | Prop valve full open area |
| $A_2$ | 0.264 $cm^2$ | Drain valve full open area |
| $A_3$ | 0.0962 $cm^2$ | Purge valve full open area |

To validate the hydrogen supply system model, this paper compares the flow rates at the anode inlet and outlet of the simulation model with data from an actual 120kW fuel cell system, as shown in Figure 5. The model accurately reflects the real system's dynamic response, capturing trends in flow rate and pressure under various conditions.

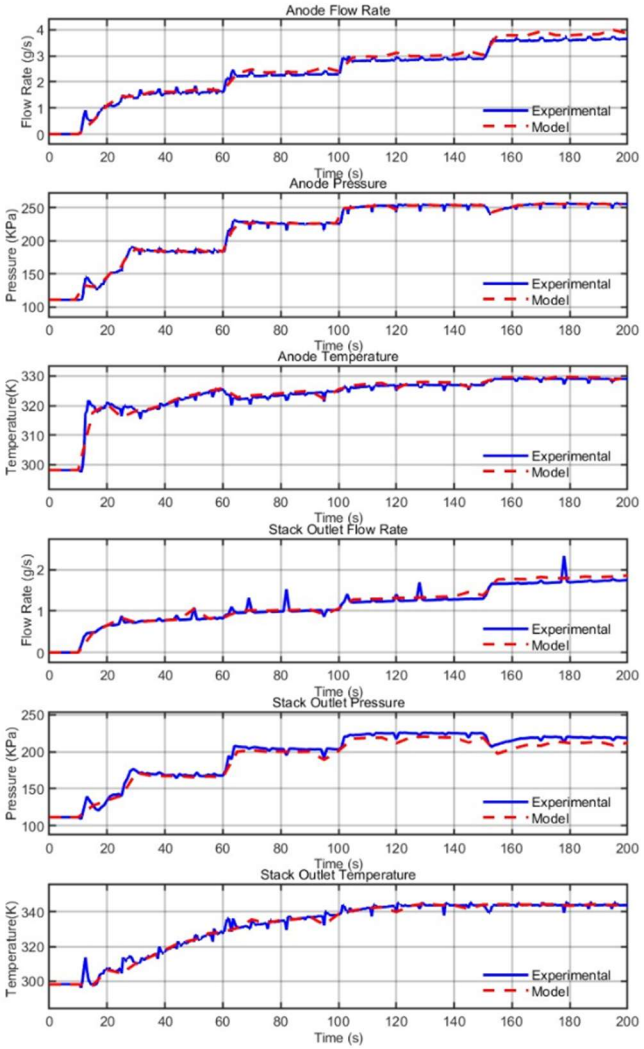

Fig. 5: Comparison between model and Experimental Results

## 5 Conclusion

This paper constructs a high-precision dynamic model integrating multi-physical field coupling characteristics. The model fully considers the composition of mixed gas, gas flow characteristics, and electrochemical reaction processes, effectively simulating the dynamic behavior of the hydrogen supply system. Additionally, a semi-physical simulation platform based on the RT-Linux system is established, and the model's reliability is verified using hardware-in-the-loop technology and real-time data interaction mechanisms. Results show that the model accurately captures the dynamic characteristics of the hydrogen supply system, including pressure fluctuations, flow responses, and changes in gas composition. This study provides key technical support for the development of PEMFC hydrogen supply system control strategies and system optimization, distributed energy, and other fields.

## 6 Acknowledgements

This research was supported by the Yuxiu Innovation Project of NCUT (Project No. 2024NCUTYXCX107). The authors are grateful for the financial support and resources provided by the project, which enabled the successful completion of this study.

## 7 References

[1] Buasri P, Salameh Z M. An electrical circuit model for a proton exchange membrane fuel cell (PEMFC)[C]//2006 IEEE Power Engineering Society General Meeting. IEEE, 2006: 6 pp.

[2] Li S C, Gao C Y, Wang F C. Control and development of a PEMFC electric bicycle[C]//2014 Proceedings of the SICE Annual Conference (SICE). IEEE, 2014: 1017-1022.

[3] Putala R, Ferencey V. Hydrogen Fuel Cell System Modeling Approaches[C]//2025 Cybernetics & Informatics (K&I). IEEE, 2025: 1-7.

[4] Zhu Y, Zou J, Li S, et al. Nonlinear model predictive control of PEMFC anode hydrogen circulation system based on dynamic coupling analysis[J]. International Journal of Hydrogen Energy, 2023, 48(6): 2385-2400.

[5] Qing H, Feng Y, Zhang C, et al. Parallel structure-based decentralized model predictive control of vehicle PEMFC anode circulation system[J]. Energy, 2025, 324: 135767.

[6] Quan S, Chen J, Wang Y X, et al. A hierarchical predictive strategy-based hydrogen stoichiometry control for automotive fuel cell power system[C]//2019 IEEE Vehicle Power and Propulsion Conference (VPPC). IEEE, 2019: 1-5.

[7] Xu K, Chen L, Dong Z, et al. Data-driven prediction of ejector performance for PEMFC hydrogen fuel recirculation system[C]//2023 IEEE 6th International Conference on Big Data and Artificial Intelligence (BDAI). IEEE, 2023: 35-39.

[8] Qin B, Wang X, Wang L, et al. Hydrogen excess ratio control of ejector-based hydrogen recirculation PEM fuel cell system[C]//2019 34rd youth academic annual conference of Chinese association of automation (YAC). IEEE, 2019: 648-653.

[9] Hauck M, Petzke F, Streif S. Model predictive purge control for PEM fuel cell systems with anode recirculation[C]//2021 60th IEEE Conference on Decision and Control (CDC). IEEE, 2021: 6359-6364.

[10] Nikiforow K, Koski P, Karimäki H, et al. Designing a hydrogen gas ejector for 5 kW stationary PEMFC system–CFD-modeling and experimental validation[J]. International Journal of Hydrogen Energy, 2016, 41(33): 14952-14970.

[11] Li G, Yuan Y, Tong L. Modeling and control study of hydrogen system for port hydrogen equipment[C]//2023 7th International Conference on Transportation Information and Safety (ICTIS). IEEE, 2023: 1-7.

[12] U. S. S. of Documents, National Institute of Standards and Technology. US Government Printing Office, 1992.